sustainability

MDPI

Article

Bi-Level Interactive Optimization of Distribution Network–Agricultural Park with Distributed Generation Support

Ke Xu [1,2], Chang Liu [1,2], Shijun Chen [3], Weiting Xu [1,2], Chuan Yuan [3], Dengli Jiang [3], Peilin Li [4,*] and Youbo Liu [4]

[1] State Grid Sichuan Electric Power Company Economic and Technological Research Institute, Chengdu 610041, China
[2] Sichuan New Power System Research Institute Co., Ltd., Chengdu 610041, China
[3] State Grid Sichuan Electric Power Company, Chengdu 610041, China
[4] School of Electrical Engineering, Sichuan University, Chengdu 610065, China
* Correspondence: 2022223030012@stu.scu.edu.cn

Abstract: The large-scale integration of renewable energy and the use of high-energy-consuming equipment in agricultural parks have a great influence on the security of rural distribution networks. To ensure reliable power delivery for residential and agricultural activities and sustainable management of distributed energy resources, this paper develops a distributed generation-supported interactive optimization framework coordinating distribution networks and agricultural parks. Specifically, a wind–photovoltaic scenario generation method based on Copula functions is first proposed to characterize the uncertainties of renewable generation. Based on the generated scenario, a bi-level interactive optimization framework consisting of a distribution network and agricultural park is constructed. At the upper level, the distribution network operators ensure the security of the distribution network by reconfiguration, coordinated distributed resource dispatch, and dynamic price compensation mechanisms to guide the agricultural park's electricity consumption strategy. At the lower level, the agricultural park users maximize their economic benefits by adjusting controllable loads in response to price compensation incentives. Additionally, an improved particle swarm optimization combined with a Gurobi solver is proposed to obtain equilibrium by iterative solving. The simulation analysis demonstrates that the proposed method can reduce the operation costs of the distribution network and improve the satisfaction of users in agricultural parks.

Keywords: interactive method; distribution network operators; agricultural Park; bi-level model; distributed resources

check for updates

Academic Editor: Francesco Riganti Fulginei

Received: 21 April 2025
Revised: 29 May 2025
Accepted: 4 June 2025
Published: 5 June 2025

Citation: Xu, K.; Liu, C.; Chen, S.; Xu, W.; Yuan, C.; Jiang, D.; Li, P.; Liu, Y. Bi-Level Interactive Optimization of Distribution Network–Agricultural Park with Distributed Generation Support. *Sustainability* **2025**, *17*, 5228. https://doi.org/10.3390/su17115228

Copyright: © 2025 by the authors. Licensee MDPI, Basel, Switzerland. This article is an open access article distributed under the terms and conditions of the Creative Commons Attribution (CC BY) license (https://creativecommons.org/licenses/by/4.0/).

1. Introduction

Under the guidance of the Dual Carbon Goals, the energy trilemma encompassing security, accessibility, and sustainability has emerged as a critical global issue [1]. In recent years, modern agricultural parks, primarily focused on greenhouse cultivation, have become widespread in rural areas [2–5]. The deployment of high-energy-consuming equipment in these parks has significantly impacted the safe operation of rural distribution networks [6–9]. To meet the security and reliability requirements of electricity supply for agricultural production and residential activities in agricultural parks, it is necessary to develop an interactive optimization method to guide agricultural parks in adjusting their electricity consumption strategies to ensure the safe and reliable operation of the distribution network.

Currently, existing research has been conducted on the operational optimization of distribution networks following the integration of renewable energy. References [10,11] studied source–load–storage coordination optimization methods under high renewable energy penetration, but they mainly focus on improving the distribution network's accommodation capacity for distributed energy resources without addressing its operational security issues. Reference [12] investigated a two-stage voltage control strategy for distribution networks with high PV penetration, but voltage regulation is only one aspect of distribution network optimization, and many other operational security indicators remain unconsidered. Reference [13] proposed a dynamic energy storage allocation and line expansion planning method for distribution networks. Although the approach considered operational security metrics, such as voltage stability and peak-to-valley load differences, its analysis of diversified renewable energy accommodation capacity was insufficient. The interaction between distribution networks and demand-side flexible resources is currently a key research direction in academia. Reference [14] addresses the impact of disordered charging of large-scale grid-connected electric vehicles on the stable operation of distribution networks, proposing a two-layer coordinated optimal scheduling method for electric vehicles and distribution networks that considers demand response and carbon quotas, which effectively reduces distribution network losses. Reference [15] proposes a low-carbon economic dispatch model for distribution networks based on carbon emission flow theory. Experimental results show that the proposed low-carbon dispatch model can effectively reduce carbon emissions while ensuring economic performance. The above references only focus on improving distribution network operation indicators and do not investigate the economic benefits brought to users. References [16–18] enhanced distribution network security by leveraging the flexibility of distributed wind, photovoltaics, and energy storage resources while maintaining renewable energy accommodation capacity. However, their studies lacked in-depth economic analysis of grid investments and insufficiently explored demand-side flexible resources. A common limitation across these studies is that they mainly focus on urban distribution networks without dedicated research on flexible load resources such as agricultural parks.

Meanwhile, domestic and foreign scholars have primarily focused their research on agricultural loads on the electrification modeling of agricultural loads or the planning methods of integrated energy systems in agricultural parks [19–21]. Reference [22] analyzed the impact of facility agriculture safety indicators on energy system security based on an environmental regulation load model for facility agriculture. However, this study only addressed the reliable operation of agricultural parks without considering their influence on the distribution network. Reference [23] developed a collaborative optimization model for waste incineration and renewable energy, proposing a rural multi-energy system optimization method for energy self-sufficiency and waste treatment. The research demonstrated that this approach could improve operational economics but did not investigate its impact on the operational security of the distribution network. Reference [24] introduced an energy management strategy for agricultural parks that considers market clearing. This study enhanced both the economic efficiency of distribution network operation and its accommodation capacity for distributed resources. Nevertheless, the accommodation capacity of distributed resources is only one of the indicators for the secure operation of the distribution network. This research did not explore more compelling operational security indicators, such as voltage and peak–valley load difference in the load curve.

The novelty and uniqueness of this study are that we propose an interactive optimization method between the distribution network and agricultural parks, which balances both the operational security of the distribution network and the production economics of agricultural users and formulates it as a bi-level optimization model to obtain the so-

lution. Furthermore, to mitigate the impact of the model's uncertainty from distributed renewable energy, we also propose a wind–photovoltaic scenario generation method based on Copula functions.

This paper has made contributions in the following aspects:

(1) We propose a wind–photovoltaic scenario generation method which considers both randomness and correlation of renewable energy power generation. This method first employs non-parametric kernel density estimation to generate the probability density functions of wind and photovoltaic power, then constructs a joint probability distribution function using Copula functions. Subsequently, we generate the marginal distribution functions of wind and photovoltaic power through Monte Carlo sampling, calculate the inverse functions, and perform clustering to obtain the final wind–photovoltaic scenario set. This approach effectively reduces the impact of the randomness and correlation of wind and photovoltaic power on subsequent model solutions.

(2) We propose an interactive optimization model between the distribution network and agricultural parks that balances both the operational security of the distribution network and the production economics of agricultural users. The DSO guides agricultural parks to adjust their electricity consumption strategies through distribution network reconfiguration, utilization of distributed resources, and electricity price compensation, thereby ensuring the secure and reliable operation of the distribution network. Agricultural users, in turn, accept price incentives to modify their electricity strategies, enhancing their own economic benefits. Under this model, both the DSO and users achieve mutual gains, fostering active interaction for a win–win solution.

(3) We establish a reliable bi-level optimization model for the distribution network and agricultural parks along with its solution method. The DSO acts as the upper-level leader in the bilevel model, while agricultural users are the lower-level followers. The operational strategies of the DSO decisively influence the electricity consumption strategies of agricultural users and, conversely, the users' strategies feedback to the DSO, prompting adjustments in its operational decisions. By employing the proposed intelligent algorithm to assist the Gurobi solver, the equilibrium solution of the model can be efficiently computed.

2. Interaction Mode Between Distribution Network and Agricultural Park

This paper takes a typical rural 10 kV distribution network as the research object, considering the integration of distributed photovoltaic, wind power, and energy storage devices, and explores the interaction relationship between distribution network operators and agricultural park users. The DSO and agricultural parks are two entities with divergent objectives. The DSO can guide agricultural parks to modify their electricity consumption strategies through distribution network reconfiguration, utilization of distributed resources like wind–PV-storage systems, and electricity price compensation mechanisms, aiming to achieve minimum comprehensive operational costs for the entire distribution network. However, agricultural park users primarily focus on their own production and operational benefits. They will only actively respond to the DSO's electricity price compensation strategy if modifying their electricity consumption patterns according to the compensation prices proves profitable. Therefore, the decision-making objective of agricultural park users is to maximize their own benefits or satisfaction levels. The distribution network operator ensures the safe and reliable operation of the distribution network through network reconfiguration, utilization of distributed resources, and provision of electricity price compensation to guide agricultural parks in adjusting their electricity consumption strategies. Agricultural park users accept the electricity price compensation to modify their electricity

consumption strategies, thereby maximizing their own benefits. The physical structure of the rural distribution network is designed as shown in Figure 1.

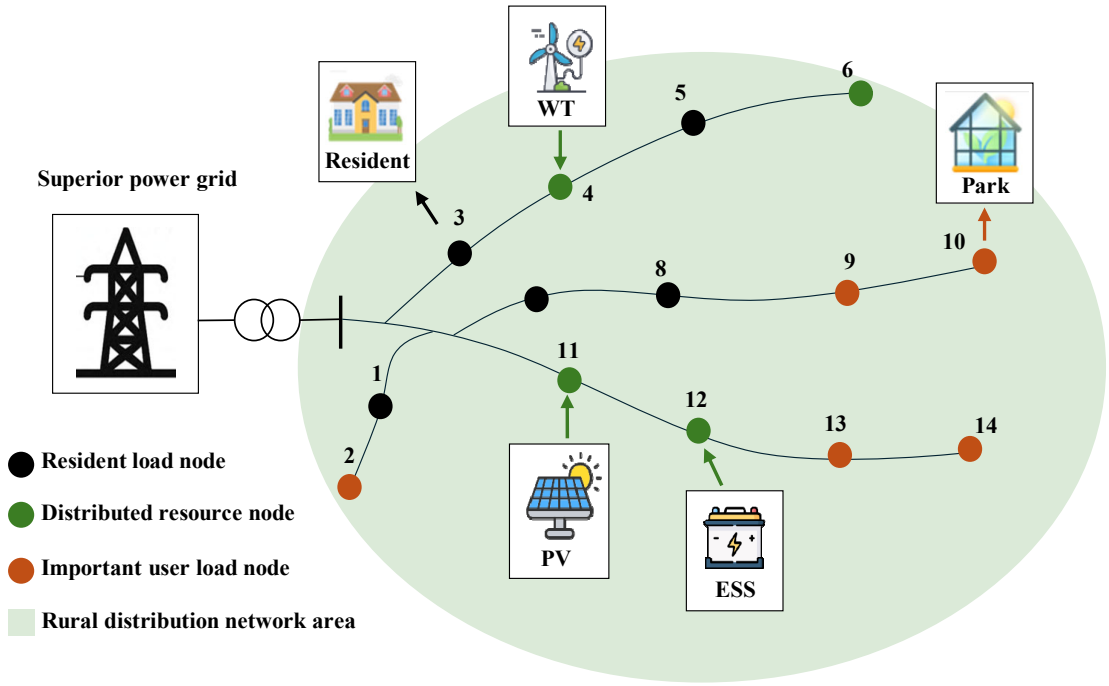


Figure 1. Schematic diagram of physical structure of rural distribution network.

Based on the above structure, the interaction mode between the distribution network and agricultural parks needs to address the following two issues: (1) how to mitigate the impact of uncertainties in wind and solar power outputs; (2) how to establish a reasonable interaction model to reduce the operational costs of the distribution network while improving the benefits of rural users.

For the first issue, this paper considers the randomness and correlation of wind and solar power outputs in the same region. Non-parametric kernel density estimation and Copula functions are used to calculate the joint probability distribution of wind and solar power outputs and scenario clustering methods are employed to generate typical wind and solar output scenarios. The details are introduced in Section 3 of this paper.

For the second issue, this paper constructs a bi-level optimization model for the distribution network and agricultural park, as shown in Figure 2. The distribution network operator and the agricultural park are two entities with different decision-making objectives. The upper-level distribution network operator guides the agricultural park in adjusting its electricity consumption strategies through network reconfiguration, utilizing distributed resources such as wind, solar, and storage, and provisioning electricity price compensation. The decision-making objective is to minimize comprehensive operational costs, including peak–valley difference costs, wind and solar curtailment costs, network loss costs, switching action costs, and electricity price compensation costs. The lower-level agricultural park users adjust their electricity consumption strategies based on the compensation electricity prices issued by the distribution network operator, with the decision-making objective being to maximize user comprehensive satisfaction, which is related to the improvement of user benefits. The details are introduced in Section 4 of this paper.

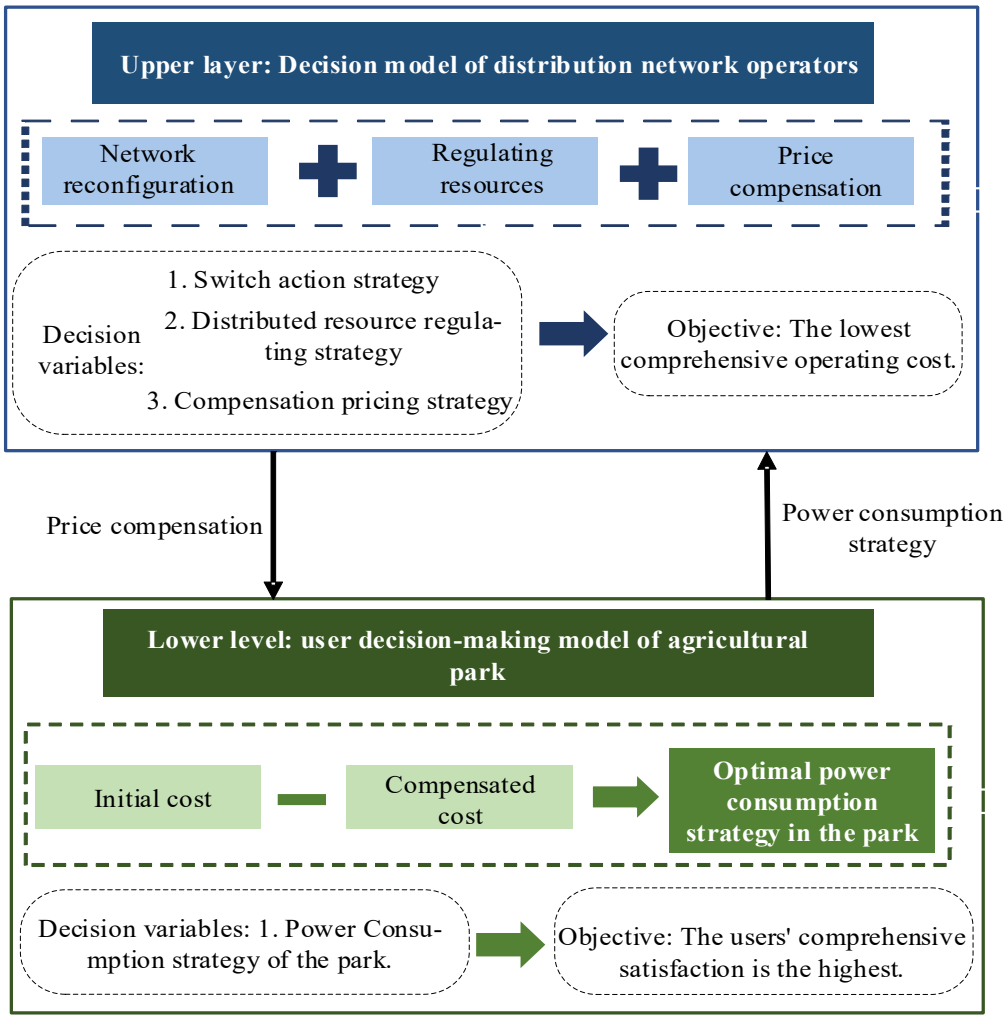


Figure 2. Double-layer optimization model of distribution.

3. Scenario Generation of Wind and Solar Power Outputs Considering Randomness and Correlation

Current mainstream methods for generating wind and photovoltaic scenarios are primarily based on statistical principles using Weibull and Beta distributions to sample wind speed and solar irradiance, respectively, thereby generating wind and photovoltaic output scenarios. However, the outputs of wind farms and photovoltaic power stations in the same region often exhibit strong statistical patterns and correlations. To ensure the effectiveness of the interaction model between the distribution network and agricultural parks, this paper considers the correlation between wind and solar power outputs in its model construction, as shown in Figure 3.

First, non-parametric kernel density estimation is used to generate the probability density functions of wind and photovoltaic power for 24 time periods. Then, the Copula function is employed to establish the joint probability distribution function of wind and photovoltaic power outputs for each time period. The mathematical expressions are as follows:

$$f(x) = \frac{1}{n_x h_x} \sum_{i=1}^{n} K_x \left(\frac{x - X_i}{h_x} \right) \quad (1)$$

$$f(y) = \frac{1}{n_y h_y} \sum_{i=1}^{n} K_y \left(\frac{y - Y_i}{h_y} \right) \quad (2)$$

$$F^T\left(x^T, y^T\right) = C\left(F_{X^T}\left(x^T\right), F_{Y^T}\left(y^T\right)\right) \tag{3}$$

$$K_x(u_x) = \frac{1}{\sqrt{2\pi}} e^{\frac{-u_x{}^2}{2}} \tag{4}$$

$$u_x = (x - X_i)/h_x \tag{5}$$

$$K_y(u_y) = \frac{1}{\sqrt{2\pi}} e^{\frac{-u_y{}^2}{2}} \tag{6}$$

$$u_y = (y - Y_i)/h_y \tag{7}$$

where $f(x)$ and $f(y)$ are the probability density functions of wind and photovoltaic power, respectively; X_i and Y_i are the actual wind and photovoltaic power outputs; x and y are the independent variables for kernel density estimation of wind and photovoltaic power; n_x and n_y are the sample sizes; h_x and h_y are the bandwidths; $Kx(\cdot)$ and $Ky(\cdot)$ are the Gaussian kernel functions for wind and photovoltaic power, respectively; T represents 24 time periods; $F^T(x^T, y^T)$ denotes the joint probability distribution function of wind and photovoltaic power for time period T; $F_{X^T}\left(x^T\right)$ represents the marginal distribution function of wind power for time period T; $F_{Y^T}\left(y^T\right)$ represents the marginal distribution function of photovoltaic power for time period T, $C(\cdot)$ is the copula connection function.

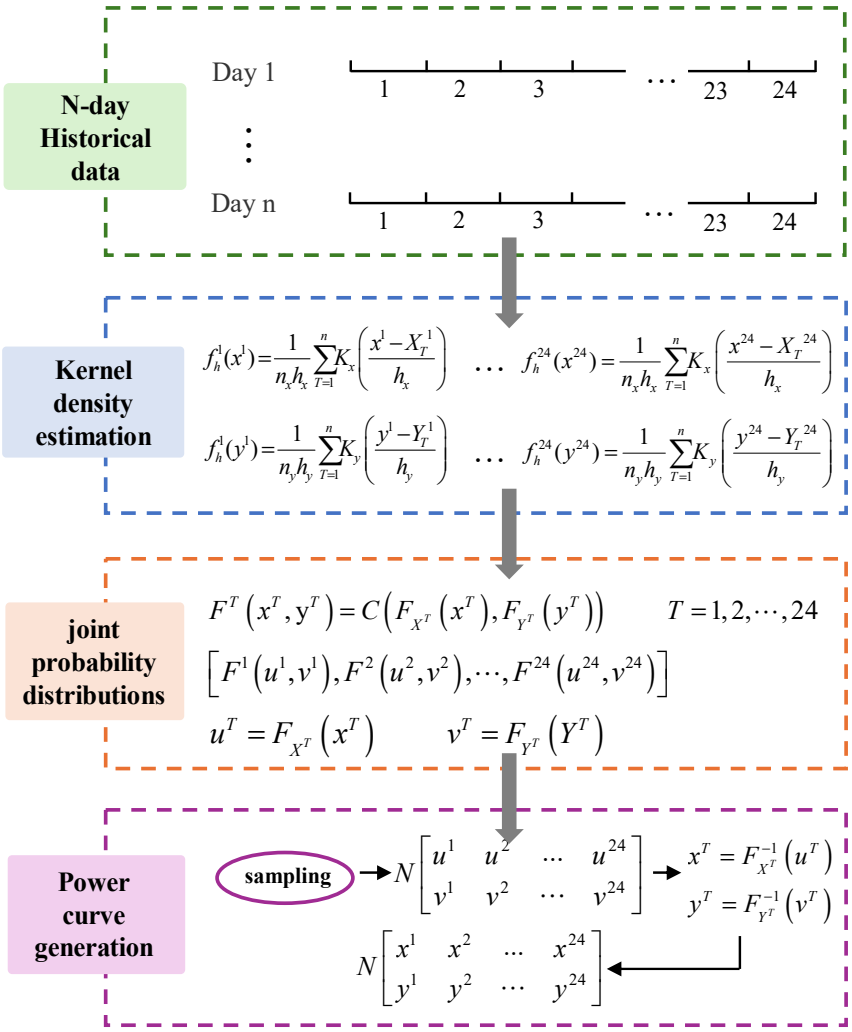


Figure 3. Generating steps of wind and light output curve.

The two common Copula families mainly include the elliptical Copula function family (Gaussian Copula, t Copula) and the Archimedean Copula function family (Frank Copula, Gumbel Copula, Clayton Copula). Since different Copula functions possess distinct fitting parameters, selecting the most suitable Copula function for characterizing wind–solar characteristics becomes crucial. This paper introduces Kendall's rank correlation coefficient and Spearman's rank correlation coefficient from the perspective of correlation. To prevent potential significant errors caused by the geometric properties of raw data, the Wasserstein distance evaluation metric is introduced from the perspective of goodness-of-fit. The correlation evaluation metrics for samples will also be calculated. Through comparative analysis, this paper selects the Frank Copula function as the optimal Copula function, with detailed results to be presented in the Section 5.

Finally, Monte Carlo sampling is used to generate the marginal distribution function of wind power, and the photovoltaic marginal distribution function is solved based on the joint probability distribution function of wind and solar power. The inverse function is then used to calculate the actual wind and photovoltaic power outputs considering temporal correlation. The mathematical expressions are as follows:

$$\frac{\partial C(u_T, v_T)}{\partial u_T} = v_T \tag{8}$$

$$x^T = F_{X^T}^{-1}(u_T) \tag{9}$$

$$y^T = F_{Y^T}^{-1}(v_T) \tag{10}$$

where $C(u_T, v_T)$ represents the joint probability distribution function of wind and photovoltaic power; u_T and v_T represent the marginal distribution function values of wind and photovoltaic power for time period T, respectively; x^T and y^T represent the actual wind and photovoltaic power outputs at time T; $F_{X^T}^{-1}(u_T)$ and $F_{Y^T}^{-1}(v_T)$ represent the inverse functions of the marginal distribution functions of wind and photovoltaic power for time period T, respectively.

The large number of wind–solar joint output curves generated by sampling with high similarity requires the application of clustering algorithms for the effective merging of similar scenarios. Among these, the partition-based k-means clustering algorithm, as a traditional clustering method, is applicable to large-scale raw scenarios. However, the initial cluster centers and the number of cluster centers are critical influencing factors for the k-means algorithm that often require manual specification, resulting in unstable clustering results. The Clustering by Fast Search and Find of Density Peaks (CFSFDP) algorithm is a clustering method that effectively determines cluster centers and quantities based on sample density, with its advantage lying in automatically identifying cluster center positions and quantities [25].

Therefore, this study follows the approach outlined in Reference [25], integrating the CFSFDP algorithm and k-means algorithm to construct an E-C-K-means clustering algorithm for effective scenario merging. The algorithmic steps are illustrated in Figure 4.

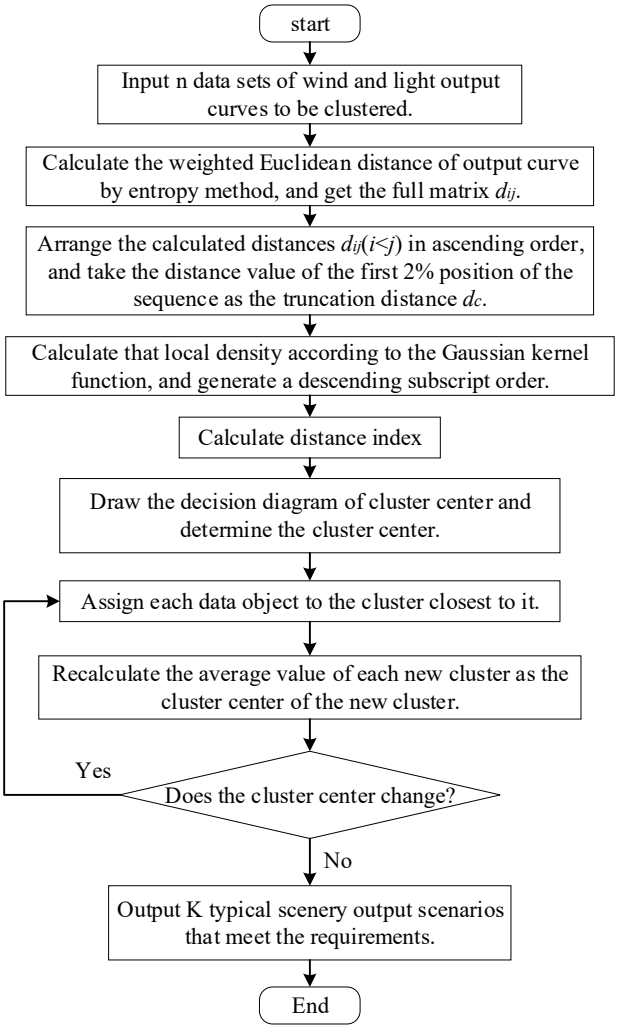


Figure 4. E-C-K-means clustering algorithm steps.

4. Bi-Level Optimization Model for Distribution Network and Agricultural Park

4.1. Optimization Model for Distribution Network Operator

4.1.1. Objective Function

The upper-level distribution network operator guides the agricultural park in adjusting its electricity consumption strategies through network reconfiguration, utilization of distributed resources, and provision of electricity price compensation. The objective function is to minimize the average comprehensive operational cost of the distribution network across all scenarios.

$$F = \sum_{s \in S} g_s (C_{FG,s} + C_{DG,s} + C_{WS,s} + C_{KG,s} + C_{BC,s}) \tag{11}$$

$$C_{FG,s} = c_{fg} \frac{\max\limits_t \left\{ \sum_{i=1}^{N} P'_{i,t,s} \right\} - \min\limits_t \left\{ \sum_{i=1}^{N} P'_{i,t,s} \right\}}{\max\limits_t \left\{ \sum_{i=1}^{T} P'_{i,t,s} \right\}} \tag{12}$$

$$C_{DG,s} = \sum_t \sum_{i \in D} c_{dg} \left(P_{i,t,s}^{dg0} - P_{i,t,s}^{dg} \right) \tag{13}$$

$$C_{WS,s} = \sum_t \sum_{j \in L} c_{ws} r_{ij} I_{ij,t,s}^{sqr} \tag{14}$$

$$C_{KG,s} = \sum_{ij \in L} c_{kg} |z_{ij,s} - z_{ij,0,s}| \tag{15}$$

where F is the comprehensive operational cost of the distribution network; S is the set of generated wind and solar power scenarios; g_s is the occurrence probability of scenario s; $C_{FG,s}$, $C_{DG,s}$, $C_{WS,s}$, $C_{KG,s}$ and $C_{BC,s}$ are the peak–valley difference cost, wind and solar curtailment cost, network loss cost, switching cost, and electricity price compensation cost of the distribution network operator for scenario s, respectively; c_{fg}, c_{dg}, c_{ws} and c_{kg} are the unit cost coefficients for peak–valley difference, wind and solar curtailment, network loss, and switching actions, respectively; N is the total number of nodes; T is the total time period; $P'_{t,i,s}$ is the net load value of node i at time t; D is the set of nodes with distributed power sources; $P^{dg0}_{i,t,s}$ and $P^{dg}_{i,t,s}$ are the output power and actual injected power of the distributed power source, respectively; r_{ij} is the resistance value; $I^{sqr}_{ij,t}$ is the square of the current; L is the set of lines; and $z_{ij,s}$ and $z_{ij,0,s}$ represent the switch states before and after network reconfiguration, respectively.

4.1.2. Constraints

(1) Distributed Power Output Constraints

$$0 \leqslant P^{dg}_{i,s} \leqslant \sum_{i \in D} \alpha^{dg}_i P^{dg}_{i,\max} \tag{16}$$

$$\sum_{i \in D} \alpha^{dg}_i Q^{dg}_{i,\min} \leqslant Q^{dg}_{i,s} \leqslant \sum_{i \in \{P\}} \alpha^{dg}_i Q^{dg}_{i,\max} \tag{17}$$

$$Q^{dg}_{i,max,s} = \sqrt{\left(S^{dg}_i\right)^2 - \left(P^{dg}_{i,s}\right)^2} \tag{18}$$

$$Q^{dg}_{i,min,s} = -\sqrt{\left(S^{dg}_i\right)^2 - \left(P^{dg}_{i,s}\right)^2} \tag{19}$$

where α^{dg}_i is a Boolean variable, with a value of 1 indicating that a distributed power source is connected to node i; $P^{dg}_{i,\max}$ represents the maximum active power; $Q^{dg}_{i,\max}$ and $Q^{dg}_{i,\min}$ represent the maximum and minimum reactive power, respectively; S^{PV}_i is the inverter capacity of node i.

(2) Energy Storage Device Charging and Discharging Constraints

$$0 \leqslant P^{\mathrm{Ech}}_{i,t,s} \leqslant U^{\mathrm{Ech}}_{i,t,s} P^{\mathrm{Ech}}_{i,\max} \tag{20}$$

$$0 \leqslant P^{\mathrm{Edch}}_{i,t,s} \leqslant U^{\mathrm{Edch}}_{i,t,s} P^{\mathrm{Edch}}_{i,\max} \tag{21}$$

$$U^{\mathrm{Ech}}_{i,t} + U^{\mathrm{Edch}}_{i,t} \leqslant 1 \tag{22}$$

$$E^{\mathrm{E}}_{i,t+\Delta t} = E^{\mathrm{E}}_{i,t} + P^{\mathrm{Ech}}_{i,t} \eta^{\mathrm{Ech}}_i \Delta t - \frac{P^{\mathrm{Edch}}_{i,t}}{\eta^{\mathrm{Edch}}_i} \Delta t \tag{23}$$

$$E^{E}_{i,\min} \leqslant E^{E}_{i,t} \leqslant E^{E}_{i,\max} \tag{24}$$

where $U^{\mathrm{Ech}}_{i,t,s}$ and $U^{\mathrm{Edch}}_{i,t,s}$ are Boolean variables, with a value of 1 indicating that the energy storage device is in charging or discharging state at time t for scenario s; $P^{\mathrm{Ech}}_{i,t,s}$ and $P^{\mathrm{Edch}}_{i,t,s}$ are the charging and discharging power of the energy storage device, respectively; $P^{\mathrm{Ech}}_{i,\max}$ and $P^{\mathrm{Edch}}_{i,\max}$ are the upper limits of the charging and discharging power of the energy storage device; η^{Ech}_i and η^{Edch}_i are the charging and discharging efficiencies of the energy storage device, respectively; $E^{E}_{i,\max}$ and $E^{E}_{i,\min}$ are the upper and lower limits of the energy storage device capacity.

(3) Capacitor Switching Constraints

$$\begin{cases} Q_{i,t,s}^{\mathrm{CB}} = N_{i,t}^{\mathrm{CB}} \times Q_{i,st}^{\mathrm{CB}} \\ N_{i,t,s}^{\mathrm{CB}} \le N_{max}^{\mathrm{CB}} \end{cases} \tag{25}$$

where $Q_{i,t,s}^{\mathrm{CB}}$ is the reactive power compensation capacity of the capacitor at node i for time t in scenario s; $Q_{i,st}^{\mathrm{CB}}$ is the reactive power compensation capacity of a single capacitor; $N_{i,t}^{\mathrm{CB}}$ is the number of capacitors switched; N_{max}^{CB} is the maximum number of capacitors that can be switched.

(4) Power Balance Constraints of the Distribution Network

$$m_{ij,s} = (1 - z_{ij,s})M \tag{26}$$

$$\sum P_{ij,s} - \sum P_{jk,s} - \sum r_{ij} I_{ij,s}^{sqr} = P_{i,s}^{new} - P_{i,s}^{\mathrm{DG}} - P_{i,s}^{\mathrm{Ech}} \tag{27}$$

$$\sum Q_{ij,s} - \sum Q_{jk,s} - \sum x_{ij} I_{ij,s}^{sqr} = Q_{i,s}^{new} - Q_{i,s}^{\mathrm{DG}} - Q_{i,s}^{\mathrm{Ech}} \tag{28}$$

$$V_{i,s}^{\mathrm{sqr}} - V_{j,s}^{\mathrm{sqr}} \leqslant m_{ij,s} + 2(r_{ij}P_{ij,s} + x_{ij}Q_{ij,s}) - \left(r_{ij}^2 + x_{ij}^2\right)\frac{P_{ij,s}^2 + Q_{ij,s}^2}{V_{i,s}^{sqr}} \tag{29}$$

$$V_{i,s}^{\mathrm{sqr}} - V_{j,s}^{\mathrm{sqr}} \geq -m_{ij,s} + 2(r_{ij}P_{ij,s} + x_{ij}Q_{ij,s} - \left(r_{ij}^2 + x_{ij}^2\right)\frac{P_{ij,s}^2 + Q_{ij,s}^2}{V_{i,s}^{sqr}} \tag{30}$$

$$0 \leqslant I_{ij,s}^{\mathrm{sqr}} \leqslant z_{ij,s} I_{ijmax}^{\mathrm{sqr}} \tag{31}$$

$$V_{imin}^{\mathrm{sqr}} \leqslant V_{i,s}^{\mathrm{sqr}} \leqslant V_{imax}^{\mathrm{sqr}} \tag{32}$$

$$P_{ij,s}^2 + Q_{ij,s}^2 \leqslant V_{i,s}^{\mathrm{sqr}} I_{ij,s}^{\mathrm{sqr}} \tag{33}$$

$$\left| \begin{matrix} 2P_{ij,s} \\ 2Q_{ij,s} \\ I_{ij,s}^{\mathrm{sqr}} - V_{i,s}^{\mathrm{sqr}} \end{matrix} \right|_2 \leqslant I_{ij,s}^{\mathrm{sqr}} + V_{i,s}^{\mathrm{sqr}} \tag{34}$$

where M represents a very large positive number; $P_{ij,s}$ and $P_{jk,s}$ represent the inflow and outflow power of node j for scenario s, respectively; $V_{i,s}^{sqr}$ is the square of the node voltage; x_{ij} is the line reactance; $P_{i,s}^{new}$ is the power consumption of the node user after accepting electricity price compensation; V_{imax}^{sqr} and V_{imin}^{sqr} are the upper and lower limits of the square of the voltage; I_{ijmax}^{sqr} is the upper limit of the square of the current.

(5) Topology Constraints of the Distribution Network

$$\sum_{ij \in L} Z_{ij,s} = N - \sum_{i \in \Omega_N} S_{i,s}^{vs} \tag{35}$$

$$\sum_{jk \in L} F_{jk,s} - \sum_{ij \in L} F_{ij,s} = F_{i,s}^{vs} - 1 \tag{36}$$

$$-S_{i,s}^{vs} M \leqslant F_{i,s}^{vs} \leqslant S_{i,s}^{vs} M \tag{37}$$

$$-z_{ij,s} M \leqslant F_{ij,s} \leqslant z_{ij,s} M \tag{38}$$

where Ω_N is the set of nodes; N is the number of nodes; $S_{i,s}^{VS}$ is a Boolean variable indicating the virtual node flag; $F_{jk,s}$ and $F_{ij,s}$ are the virtual power flows of the branches; $F_{i,s}^{\mathrm{vs}}$ is the virtual power emitted by node i.

(6) Compensation Electricity Price Constraints

$$\Delta\delta_t^{\mathrm{bc}} = \lambda\delta_t^0 \tag{39}$$

$$\lambda_{min} \le \lambda \le \lambda_{min} \tag{40}$$

where $\Delta\delta_t^{bc}$ is the compensation electricity price set by the distribution network operator at time t; λ is the compensation electricity price coefficient; δ_t^0 is the basic electricity price at time t; λ_{min} and λ_{max} are the lower and upper limits of the compensation electricity price coefficient.

4.2. Optimization Model for Agricultural Park Users

4.2.1. Objective Function

Agricultural park users adjust their electricity consumption strategies based on the compensation electricity prices issued by the distribution network operator. The satisfaction level is influenced by the degree of benefit improvement and individual satisfaction differences.

$$f = \sum_{s \in S} \frac{(f_{u,s}^{ave} - f_{u,s}^{min}) f_{u,s}^{ave} g_s}{(f_{u,s}^{max} - f_{u,s}^{min})} \tag{41}$$

$$f_{u,s}^{ave} = \sum_{u \in U} f_{u,s} / N_u \tag{42}$$

$$f_{u,s} = C_{BC,s} / \rho \sum_t \delta_t^0 P_{u,t,s}^{ws0} \tag{43}$$

$$C_{BC,s} = (\sum_t \delta_t^0 P_{u,t,s}^{load} - \sum_t \left(\delta_t^0 - \Delta\delta_t^{bc}\right) P_{u,t,s}^{new}) \tag{44}$$

where f is the comprehensive user satisfaction index; $f_{u,s}^{ave}$, $f_{u,s}^{max}$ and $f_{u,s}^{max}$ are the average user satisfaction and its lower and upper limits for scenario s, respectively; $f_{u,s}$ is the satisfaction of user u; U is the set of agricultural park nodes; N_u is the number of agricultural park users; ρ is the benefit expectation coefficient; $P_{u,t,s}^{load}$ is the predicted power consumption of agricultural park user u; $P_{u,t,s}^{new}$ is the actual power consumption of agricultural park user u after electricity price compensation.

4.2.2. Constraints

(1) Energy Consumption Model of the Agricultural Park

Assuming the agricultural park primarily engages in greenhouse cultivation, the electricity load mainly consists of irrigation, temperature control, and supplemental lighting equipment:

$$P_{u,t,s}^{load} = n_1 P_{u,t,s}^{\text{water}} + n_2 P_{u,t,s}^{tem} + n_3 P_{u,t,s}^{\text{light}} \tag{45}$$

where $P_{u,t,s}^{\text{water}}$, $P_{u,t,s}^{tem}$ and $P_{u,t,s}^{\text{light}}$ are the power consumption of irrigation, temperature control, and supplemental lighting equipment for agricultural park user u at time t in scenario s, respectively; $n1$, $n2$, and $n3$ are the quantities of the corresponding equipment.

(2) Energy Consumption Model of Irrigation Equipment

The irrigation system primarily relies on equipment such as electric drainage and irrigation systems, sprinklers, and humidity sensors to periodically water plants. Through real-time humidity tracking and dynamic adjustments, it enhances soil moisture levels and promotes crop growth. According to Reference [26], the actual irrigation volume is calculated based on crop transpiration and evaporation rates under optimal growth conditions. Reference [27] demonstrates that the drainage volume of agricultural electric drainage systems can be determined through crop water requirements, with specific formulas as follows:

$$P_{t,s}^{\text{water}} = \sum_{h=1}^{T_w} W_{t,s}^1 / \eta_w \tag{46}$$

$$W_{t,s}^1 = W_{t,s}^2 H_w \left(\frac{\rho_w g}{3600}\right) \tag{47}$$

where T_w is the irrigation time; $W_{t,s}^1$ represents the drainage volume of electric irrigation; η_w is the efficiency of the electric irrigation pump motor; $W_{t,s}^2$ represents the evapotranspiration of crops; H_w is the pressure of the water pump; g is the gravitational acceleration; ρ_w is the density of water.

(3) Energy Consumption Model of Temperature Control Equipment

The temperature control system transmits data from electronic thermometers to the control console and adjusts the heating output of air-source heat pumps according to crop types, implementing real-time temperature adjustments to maintain optimal growth temperatures for crops. As demonstrated in Reference [28], the operational model calculation formula for the temperature control system is as follows:

$$P_{t,s}^{tem} = k_{tem} A_{tem} \frac{\Delta F_{set,s}}{\eta_{tem}} \tag{48}$$

$$\Delta F_{set,s} = \frac{Q_{n,s}}{1300} V_{tem} \tag{49}$$

where k_{tem} is the thermal conductivity coefficient of the temperature control equipment; $\Delta F_{set,s}$ represents the difference between the ideal temperature and the actual temperature; A_{tem} represents the area of the greenhouse; η_{ahb} is the thermal conversion efficiency; $Q_{n,s}$ is the total heat load loss; V_{tem} is the air volume inside the greenhouse.

(4) Energy Consumption Model of Lighting Equipment

During periods of sufficient sunlight, the photosynthetic demands of greenhouse crops can generally be met. However, during adverse weather conditions or prior to full sunrise, supplemental lighting using intelligent LED systems becomes necessary to enhance photosynthetic intensity. As established in Reference [29], the operational modeling equations for the temperature control system are formulated as follows:

$$P_{t,s}^{\text{light}} = \frac{-48}{0.0004} \left(\frac{I_{\text{light}}^{t,s}}{11.57} \right)^2 + \frac{7 * I_{\text{light}}^{t,s}}{11.57} - 0.41 \tag{50}$$

$$I_{\text{light}}^{t,s} = I_{\text{set}}^{t,s} - I_{\text{sun}}^{t,s} \tag{51}$$

where $I_{\text{light}}^{t,s}$ is the supplemental lighting intensity; $I_{\text{set}}^{t,s}$ is the ideal lighting intensity; $I_{\text{sun}}^{t,s}$ is the actual lighting intensity.

(5) Power Constraints of Agricultural Park Load

$$\sum_{t=1}^{T} P_{u,t,s}^{new} = \sum_{t=1}^{T} P_{u,t,s}^{load} \tag{52}$$

$$\sigma_{min} P_{u,t,s}^{load} \le P_{u,t,s}^{new} \le \sigma_{max} P_{u,t,s}^{load} \tag{53}$$

where $P_{u,t,s}^{new}$ is the actual power consumption of agricultural park user u at time t in scenario s after electricity price compensation; σ_{min} and σ_{max} represent the lower and upper limits of power consumption adjustment.

4.3. Solution Method for the Bi-Level Optimization Model

Considering the inconsistent decision-making objectives and mutual influence of the calculation results between the upper and lower levels of the bi-level optimization model for the distribution network and agricultural park, this paper employs an improved particle swarm optimization (PSO) algorithm [30] combined with the Gurobi solver to iteratively find the equilibrium solution of the model.

The improvement process of the traditional PSO algorithm is as follows: to overcome inherent limitations of conventional PSO algorithms, including susceptibility to local optima, insufficient convergence precision, and parameter sensitivity, this study introduces chaotic sequences and simulated annealing mechanisms to enhance the traditional PSO algorithm, establishing the Chaotic-Simulated Annealing Particle Swarm Optimization (CSAPSO) algorithm. The iterative logic of the conventional PSO algorithm operates as follows:

$$V_{md}^{k+1} = \omega V_{md}^{k} + c_1 r_1 (P_{md}^{k} - X_{md}^{k}) + c_2 r_2 (P_{pd}^{k} - X_{md}^{k}) \tag{54}$$

$$X_{md}^{k+1} = X_{md}^{k} + V_{md}^{k+1} \tag{55}$$

where k denotes the iteration count; V_{md}^{k} represents the velocity vector; X_{md}^{k} denotes the position vector; ω is the inertial parameter; P_{md}^{k} signifies the particle's best-known position; P_{pd}^{k} indicates the population's global best position; c_1 and c_2 are acceleration constants; r_1 and r_2 are random numbers uniformly distributed in [0, 1].

Observably, all particles in the population converge toward the optimal position. However, when the global optimum coincides with a local optimum, the algorithm tends to stagnate near local optima. For complex optimization problems with multiple local optima, repeated iterations often lead to premature convergence, characterized by a diminished global search capability, reduced population diversity, and eventual entrapment in locally optimal solutions.

To enhance the global exploration capacity of the PSO algorithm, this study adopts a linear decrement strategy to update the inertial parameter ω and incorporates chaotic sequences to dynamically adjust the stochastic coefficients r_1 and r_2, defined as follows:

$$\omega(k) = \omega_0 - k(\omega_0 - \omega_1)/k_{set} \tag{56}$$

$$r_t^{k+1} = \mu * r_t^k * (1 - r_t^k) \quad t = 1, 2 \tag{57}$$

where ω_0 and ω_1 represent the initial and final inertial weights of the algorithm; k_{set} denotes the predefined iteration count; and μ is the control variable, set to 4 in this study, under which the Logistic map exhibits fully chaotic behavior.

To further enable the algorithm to escape local optima, this work incorporates a simulated annealing mechanism that probabilistically accepts inferior solutions, defined as follows:

$$P_m = \frac{exp((f(P_{md}) - f(P_{pd}))/T)}{\sum_{m \in M} exp((f(P_{md}) - f(P_{pd}))/T)} \tag{58}$$

$$T = T_0 * a \tag{59}$$

$$T_0 = \frac{P_{pd}}{ln0.2} \tag{60}$$

where P_m denotes the annealing fitness of particle m; $f(P_{md})$ represents the PSO fitness of particle m; $f(P_{pd})$ indicates the population-level PSO fitness; T is the annealing temperature; T_0 signifies the initial annealing temperature; and a denotes the cooling rate.

Finally, employing the roulette wheel selection method based on the annealing fitness P_m, particle r is selected to replace the global optimum position. The updated PSO iterative formula is defined as:

$$V_{md}^{k+1} = \omega V_{md}^{k} + c_1 r_1 (P_{md}^{k} - X_{md}^{k}) + c_2 r_2 (P_{rd}^{k} - X_{md}^{k}) \tag{61}$$

where P_{rd}^{k} denotes the position of particle r selected through roulette wheel selection.

Through the aforementioned improvement process, the CSAPSO proposed in this study effectively enhances the global search capability of conventional PSO algorithms,

prevents premature convergence to local optima, and ensures more reliable computational results.

The specific workflow for iteratively seeking the equilibrium solution of the distribution network–agricultural park bi-level model using the CSAPSO algorithm integrated with the Gurobi solver is outlined as follows:

(1) Input the relevant parameters of the bi-level optimization model for the distribution network and agricultural park (including peak–valley difference of distribution network, wind and solar curtailment cost, network loss cost, switching action cost, operation parameters of wind power, photovoltaic and energy storage equipment, income expectation coefficient of users in agricultural parks, upper and lower limits of compensation electricity price, etc.), and set the parameters of the CSAPSO algorithm.
(2) Set the iteration count $k = 0$.
(3) Use the CSAPSO algorithm to randomly generate m sets of compensation electricity prices ϕ_m for the rural distribution network and pass the parameters to the user level.
(4) For the price compensation menu, the user level calls the Gurobi solver to calculate the electricity consumption plan with the goal of maximizing comprehensive satisfaction, retains the current benefits f_m^k, and returns the subscription plan to the DSO decision-making level.
(5) Based on the user subscription plan, the DSO calls the Gurobi solver to calculate the optimal distribution network reconfiguration and distributed resource utilization strategy with the goal of minimizing comprehensive operational costs and retaining the current revenue F_m^k and distribution network operation strategy ψ_m^k.
(6) Record the particle positions P_{md}, the population optimal position P_{pd}, the particle fitness F_m^k, the population optimal fitness F_{max}, and calculate the temperature T of the simulated annealing algorithm.
(7) If $k < k_{set}$, use the selection and mutation mechanism of the CSAPSO algorithm to generate new m sets of compensation electricity prices and go back to step (4), setting $k = k + 1$. If $k \geq k_{set}$, proceed to step (8).
(8) Output the optimal DSO compensation electricity price plan ϕ, distribution network operation strategy ψ, DSO comprehensive operational cost F_{min}, and user comprehensive satisfaction f_{max}.

5. Case Study

5.1. Case Description

This paper uses an improved IEEE 33-node distribution system to verify the effectiveness of the proposed strategy. The node types and connected distributed resources are shown in Figure 5, where the capacitor bank is set at node 33. The parameters of the agricultural park equipment are referenced from [24]. The time-of-use electricity price curve for the rural power grid is shown in Figure 6. The relevant parameters of the bi-level optimization model for the distribution network and agricultural park are listed in Table 1.

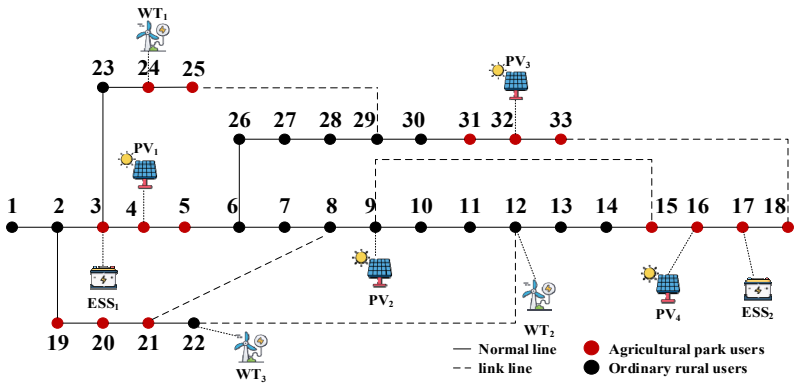


Figure 5. Improved IEEE33-bus distribution system.

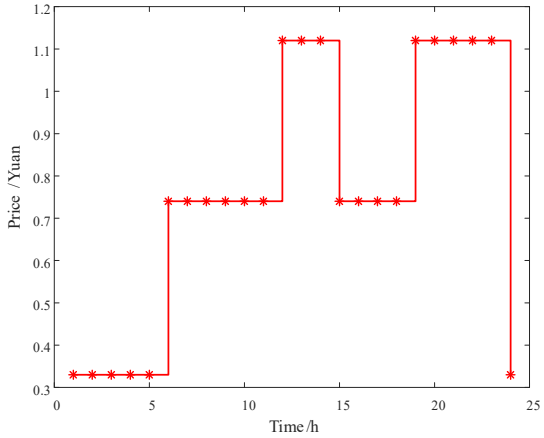


Figure 6. Time-of-use price of rural power grid.

Table 1. Relevant parameters of distribution network–agricultural park two-level optimization model.

Parameter	Description	Value	Unit
c_{fg}	Peak–valley difference cost coefficient	3000	—
c_{dg}	Wind and solar curtailment cost coefficient	5	CNY/kW
c_{ws}	Network loss cost coefficient	3	CNY/kWh
c_{kg}	Switching action cost coefficient	50	CNY/time
P_{max}^{PV}	Maximum active power of photovoltaic	400	kW
P_{max}^{WT}	Maximum active power of wind power	400	kW
P_{max}^{E}	Maximum active power of energy storage	200	kW
Q_{max}^{E}	Maximum reactive power of energy storage	170	kvar
E_{max}^{E}	Upper limit of energy storage capacity	600	kWh
$E_{\min}^{E}$	Lower limit of energy storage capacity	100	kWh
Q_{st}^{CB}	Reactive power compensation of capacitor	0.2	Mvar
N_{max}^{CB}	Total number of capacitors	4	—
η	Charging and discharging efficiency	95	%
ρ	Benefit expectation coefficient	50	%
λ_{min}	Lower limit of compensation electricity price coefficient	0.1	—
λ_{max}	Upper limit of compensation electricity price coefficient	1	—

5.2. Scenario Generation

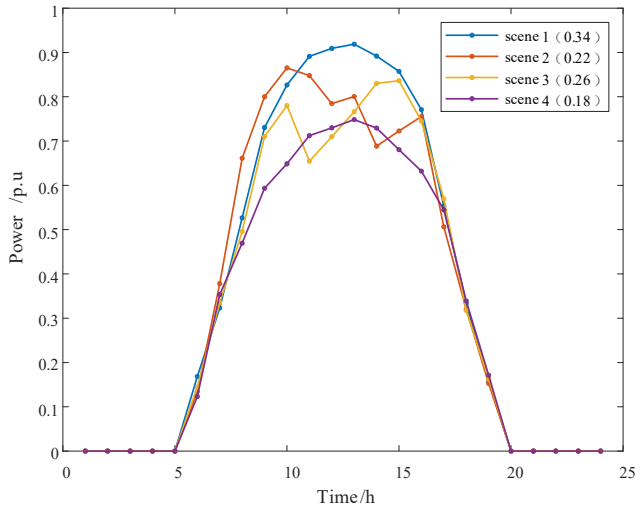
To determine the per-unit output of wind and photovoltaic units, we selected a rural area of Sichuan Province for one full year. Initially, fitting procedures were conducted using five types of Copula functions, with the evaluation metrics for each function calculated as shown in Table 2.

Table 2. Model calculation results under different function types.

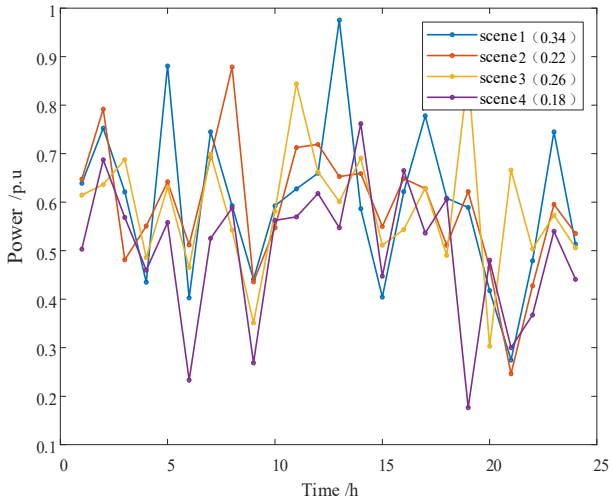
Function Type	Spearman Rank Correlation Coefficient	Kendall Rank Correlation Coefficient	Wasserstein Distance
Sample data	−0.0154	−0.0133	0
Gaussian Copula	−0.0261	−0.0303	0.0421
t Copula	−0.0513	−0.0203	0.0613
Gumbel Copula	1.0455×10^{-6}	6.1527×10^{-7}	0.0515
Clayton Copula	2.0407×10^{-6}	1.4576×10^{-6}	0.0621
Frank Copula	−0.0163	−0.0146	0.013

As evident from the table, the model exhibits differential fitting effectiveness across parameter variations of distinct Copula functions. Based on the fitting results obtained in this study, the Frank Copula function demonstrates the closest alignment with sample data and achieves optimal fitting performance. Therefore, the Frank Copula parameters are selected for model fitting in this research.

The method described in Section 2 is used to generate four typical wind and solar output scenarios, as shown in Figure 7. The occurrence probabilities of Scenario 1, Scenario 2, Scenario 3, and Scenario 4 are 0.34, 0.22, 0.26, and 0.18, respectively.



(**a**) Photovoltaic scene



(**b**) Wind power scene

Figure 7. Typical output scenes.

5.3. Case Analysis

To verify the superiority of the proposed method, five comparative cases were set up, as shown in Table 3. Among them, Case 5 did not consider the correlation between wind and solar power, i.e., conventional methods were used to generate scenarios for wind and photovoltaic power separately.

Table 3. Case setting.

Case	WT & PV	Energy Storage	Network Reconfiguration	Price Compensation	WT and PV Correlation
1	√	√	√	√	√
2	√	×	√	√	√
3	√	√	×	√	√
4	√	√	√	×	√
5	√	√	√	√	×

As shown in Table 3, Case 1 comprehensively considers distributed power supply support, energy storage device charging/discharging, distribution network topology reconfiguration, DSO's electricity price compensation mechanism, and the correlation between wind and photovoltaic power outputs. Subsequently, Case 2 neglects the flexible power support function of energy storage device charging/discharging operations based on Case 1. Case 3 ignores the role of distribution network reconfiguration on the foundation of Case 1. Case 4 eliminates the interaction between the distribution network and agricultural parks from Case 1, meaning DSO does not guide users to adjust electricity consumption strategies through price compensation mechanisms. Case 5 disregards wind–photovoltaic correlations in Case 1, instead adopting conventional methods for separate scenario generations of wind and photovoltaic power.

Case 1 represents the most comprehensively designed scenario in this study with the fullest consideration of factors. Under optimal conditions, the model calculation results of Case 1 should naturally demonstrate superior performance compared to the other four cases. However, if the distribution network operation does not activate energy storage devices, implement network reconfiguration, or enforce price compensation mechanisms or when the implementation costs of these strategies exceed their operational benefits to the grid, the model performance under Cases 2–5 might potentially outperform that of Case 1.

Therefore, in order to verify the above analysis, the CSAPSO algorithm proposed in Section 4.3 is employed for iterative solving, with the following parameter settings: the number of particles m is 80, the number of iterations k is 200, the initial inertia weight ω_0 is 0.9, the terminal inertia weight ω_1 is 0.4, the simulated annealing cooling coefficient δ is 0.93, and the Logistics mapping control variable μ = 4. The calculation results of the model are presented in Table 4.

Table 4. Calculation results of the model in different cases.

Case	Distribution Network Operation Cost/CNY	Comprehensive User Satisfaction	User Benefit/CNY
1	5012.6	92.2%	1760.4
2	5988.9	75.4%	1440.2
3	5485.7	80.7%	1540.1
4	6548.5	0	0
5	5216.9	86.9%	1660.3

A comparison of Cases 1, 2, 3, and 4 reveals that Case 1 represents the complete proposed method, which considers distributed power supply support for the interactive optimization of the distribution network and agricultural park. In contrast, Case 2 neglects the utilization of energy storage devices, Case 3 omits distribution network reconfiguration, and Case 4 does not involve the interaction between the distribution network and the agricultural park. Consequently, the comprehensive operation costs of the distribution network in Cases 2, 3, and 4 are higher than those in Case 1, while the user benefits and comprehensive satisfaction in these cases are lower than those in Case 1. Notably, Case 4 exhibits the highest comprehensive operation cost among all cases, highlighting the superiority of the proposed interactive method in reducing distribution network operation costs. Comparing the interactive optimization results of Cases 1 and 5, it is evident that considering the correlation between wind and solar power in scenario generation further reduces distribution network operation costs and enhances user satisfaction. Integrating the above analytical results conclusively demonstrates that the strategies proposed in this study—including utilizing energy storage devices, implementing network reconfiguration, and enforcing electricity price compensation mechanisms—deliver greater operational benefits to the distribution network than the costs incurred through their implementation. This is precisely why Case 1, which incorporates the most comprehensive considerations, delivers the best model calculation results among the five cases.

To visually demonstrate the improvement in distribution network operation quality achieved by the proposed method, a comparison of distribution network operation indicators under different cases is illustrated in Figure 8.

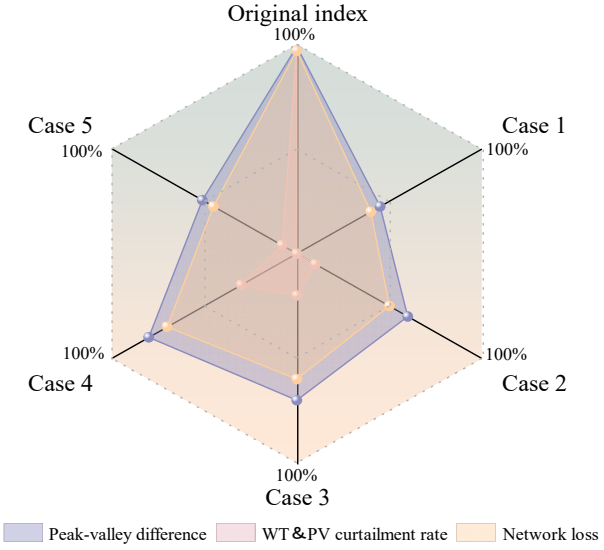


Figure 8. Comparison diagram of distribution network operation index under different cases.

From Figure 8, it can be observed that Cases 1 and 5 significantly outperform Cases 2, 3, and 4 in terms of peak–valley difference, wind and solar curtailment, and network loss indicators. This demonstrates that distribution network reconfiguration, utilization of distributed resources, and appropriate interaction methods between the distribution network and agricultural park all contribute to improving distribution network operation indicators. Case 2 slightly outperforms Case 3, indicating that in the constructed test scenario, energy storage devices have a greater impact on enhancing distribution network operation indicators than reconfiguration. Case 4 exhibits the worst performance among all cases, further underscoring the superiority of the proposed interaction method in improving distribution network reliability.

Furthermore, taking Scenario 1 under Case 1 as an example, the compensation electricity price curve and load variation curve of the distribution network are plotted in Figures 9 and 10, respectively.

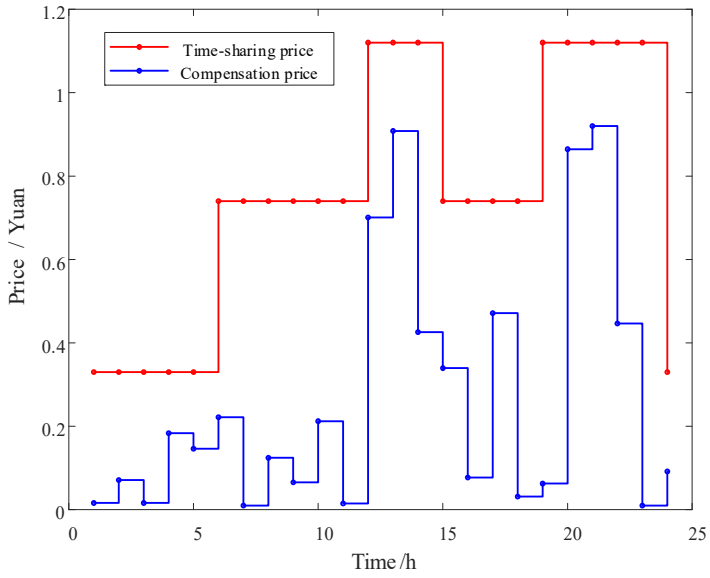


Figure 9. Compensation price curve of distribution network.

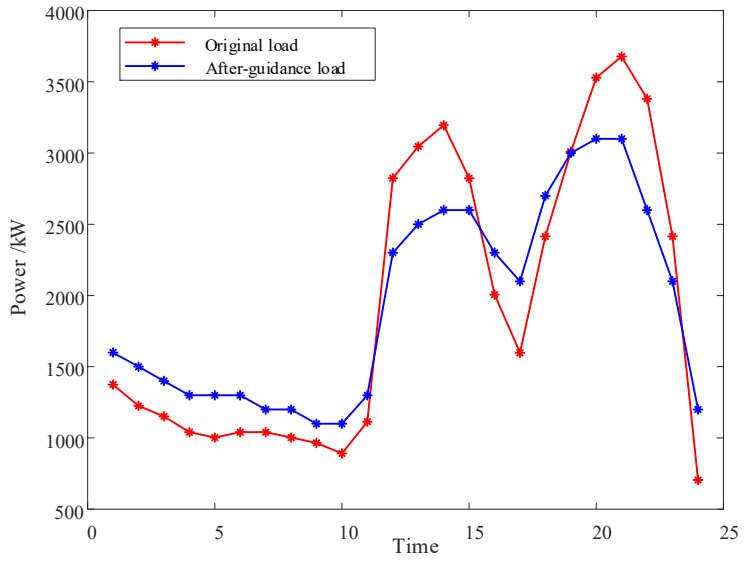


Figure 10. Distribution network load transformation curve.

A comparison of Figures 9 and 10 reveals that, after guiding agricultural parks to adjust their electricity consumption strategies through compensation pricing, part of the distribution network load shifts from 12:00–15:00 and 18:00–22:00 to 0:00–5:00, resulting in a reduction in the peak-valley difference of the load curve. Additionally, it is evident that the compensation electricity prices set by the distribution network operator during peak load periods are significantly higher than those during off-peak periods, ensuring effective guidance for agricultural park users to modify their consumption strategies.

Figure 11 presents the surface diagram of node voltage changes in the distribution network before and after the implementation of the proposed strategy for Scenario 1 under Case 1. To analyze the impact of the proposed method on node voltage during peak load periods, the voltage variation curve at 3:00 p.m. is plotted in Figure 12.

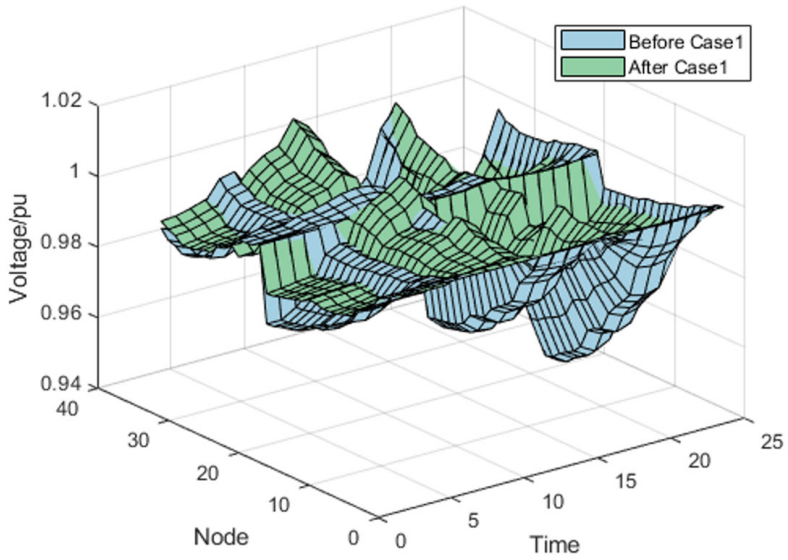


Figure 11. Curved surface diagram of node voltage change in distribution network.

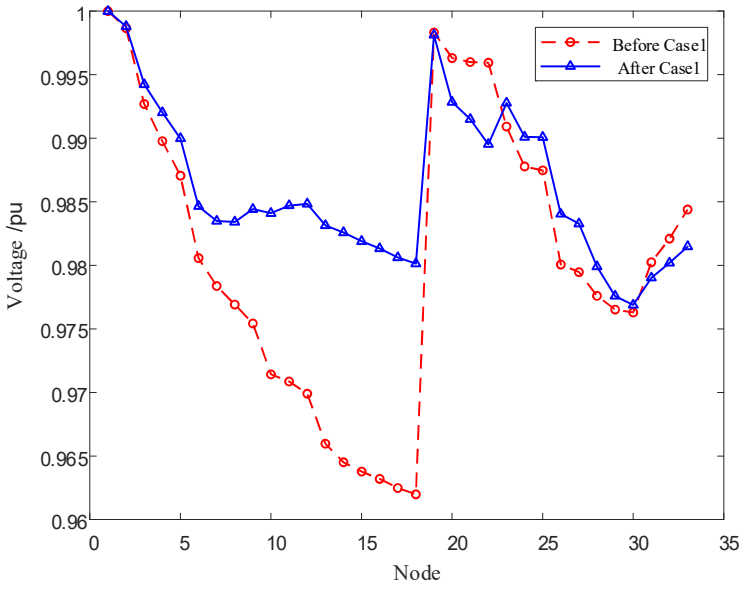


Figure 12. Voltage variation curve of distribution network nodes at 3 p.m.

From Figure 12, it can be seen that after implementing the proposed interactive optimization method, the overall voltage level of the distribution network is significantly improved. This is because, during the peak load period at 3:00 p.m., the distribution network operator guides agricultural parks to reduce their electricity consumption through compensation pricing, thereby decreasing the total load and enhancing the voltage quality. These results demonstrate the effectiveness of the proposed strategy in improving voltage quality during peak load periods.

Furthermore, to visually demonstrate the improvement magnitude of node voltages in the distribution network before and after implementing Case 1, this paper subtracts the post-Case 1 node voltage values from the pre-Case 1 values, generating a new 3D surface plot that illustrates the numerical differences between the "Before Case 1" and "After Case 1" conditions, as shown in Figure 13.

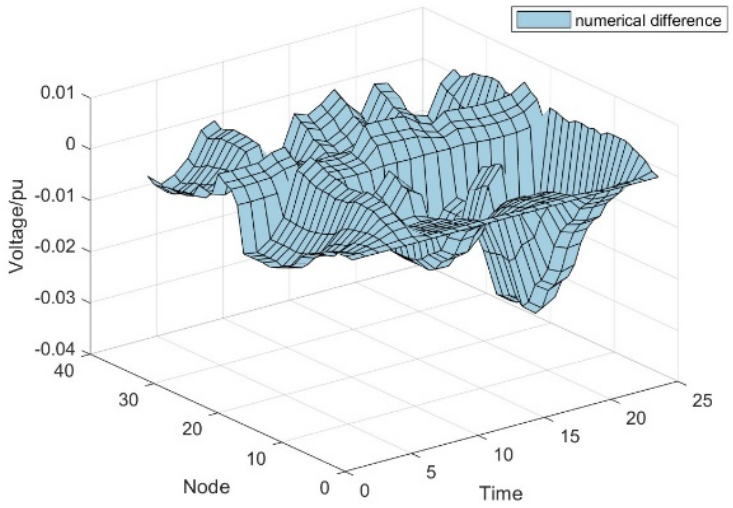


Figure 13. Improved amplitude surface diagram of distribution network node voltage.

As illustrated, the afternoon hours exhibit the most significant improvement in node voltage levels within the distribution network. This occurs because the afternoon period coincides with the peak electricity consumption phase for agricultural production and residential activities, during which the distribution network voltage typically drops to lower levels. After implementing Strategy 1, the distribution system operator (DSO) effectively reduces agricultural park electricity demand through the price compensation mechanism, thereby enhancing voltage values during the afternoon peak load period. These results collectively validate that the proposed strategies in this study effectively improve voltage quality during peak load conditions in distribution networks.

6. Conclusions

The large-scale integration of renewable energy and the deployment of high-energy-consuming equipment in agricultural parks pose significant challenges to the safe operation of rural distribution networks. To meet the demand for reliable power supply in residents' production and daily lives, we propose an interactive optimization method between distribution networks and agricultural parks that incorporates distributed power supply support. First, the correlation between wind and photovoltaic power is considered to generate scenario sets of renewable energy power generation to distribution network–agricultural park interactions. Building on this, a bi-level optimization model is established. The DSO ensures grid safety and reliability through network reconfiguration, dispatching distributed resources, and providing electricity price compensation to guide agricultural parks in adjusting their power consumption strategies. Agricultural park users accept price compensation to modify their electricity usage patterns, thereby enhancing their own operational benefits. The equilibrium solution of the model is iteratively determined using the CSAPSO algorithm combined with the Gurobi solver. Through in-depth analysis of the model and comparative case studies, the following conclusions are drawn:

(1) The proposed wind–photovoltaic scenario generation method can effectively reduce the impact of randomness and correlation between wind and PV power on model solutions. The proposed method first employs non-parametric kernel density estimation to generate probability density functions for wind and photovoltaic power outputs. It then utilizes Copula functions to establish a joint probability distribution, followed by Monte Carlo sampling to derive marginal distribution functions for wind and photovoltaic power. Finally, inverse function calculations and clustering are applied to generate the ultimate wind–photovoltaic scenario set. This approach

effectively reduces the impact of randomness and correlation between wind and photovoltaic power on subsequent model optimization. Compared to models that ignore wind–photovoltaic correlations, the proposed scenario generation method achieves lower operational costs for the DSO-controlled distribution network. Additionally, the production efficiency and quality of life benefits for agricultural park users are enhanced, with user satisfaction increasing by 5% under this framework.

(2) The proposed interactive optimization model between the distribution network and agricultural parks, which balances the operational safety of the distribution network with the production economics of agricultural users, ensures the secure and reliable operation of the distribution network through the DSO's implementation of network reconfiguration, dispatch of distributed resources, and provision of electricity price compensation to guide agricultural parks in adjusting their electricity consumption strategies. Meanwhile, agricultural park users accept the price compensation to modify their consumption strategies, thereby enhancing their own benefits. Case study analysis demonstrates that the proposed distribution network-agricultural park interactive optimization model achieves highly favorable effects in improving operational indicators such as peak–valley load difference, wind and photovoltaic curtailment, network losses, and voltage quality in the distribution network.

(3) In the proposed bi-level optimization model for the distribution network and agricultural parks, the DSO acts as the upper-level leader, while agricultural park users serve as lower-level followers. The DSO's operational strategies play a decisive role in shaping the electricity consumption strategies of agricultural users. Simultaneously, the users' consumption strategies reciprocally influence the DSO's operational decisions, prompting appropriate adjustments. By leveraging the proposed intelligent algorithm combined with the Gurobi solver, the equilibrium solution of the model can be efficiently computed. Under this framework, both the distribution system operator and users achieve mutually beneficial outcomes. Case study analysis verifies that this model achieves effective coordination between grid operation safety and user economic benefits, demonstrating significant practical value. The proposed bi-level optimization model reduces distribution network operation costs while enhancing user satisfaction in agricultural parks, achieving a balanced trade-off between the benefits of distribution network operators and agricultural park users.

Author Contributions: Formal analysis, Y.L.; investigation, C.Y. and D.J.; resources, S.C. and W.X.; writing—original draft, P.L.; writing—review and editing, K.X. and C.L. All authors have read and agreed to the published version of the manuscript.

Funding: Financial support was provided by the State Grid Sichuan Electric Power Company Science and Technology Project "Key Research on Development Path Planning and Key Operation Technologies of New Rural Electrification Construction" under Grant No. 52199623000G.

Institutional Review Board Statement: Not applicable.

Informed Consent Statement: Not applicable.

Data Availability Statement: The data presented in this study are available on request from the corresponding author.

Conflicts of Interest: The authors declare that they have no known competing financial interests or personal relationships that could have appeared to influence the work reported in this paper.

References

1. Gheorghiu, C.; Scripcariu, M.; Tanasiev, G.N.; Gheorghe, S.; Duong, M.Q. A Novel Methodology for Developing an Advanced Energy-Management System. *Energies* **2024**, *17*, 1605. [CrossRef]
2. Golmohamadi, H. Demand-Side Flexibility in Power Systems: A Survey of Residential, Industrial, Commercial, and Agricultural Sectors. *Sustainability* **2022**, *14*, 7916. [CrossRef]
3. Zhang, L.; Wu, Y.; Wang, Q. Large-scale Development of Renewable Energy in Consideration of Carbon Neutrality and Cost Optimization. *Guangdong Electr. Power* **2023**, *36*, 31–39.
4. Liao, R.; Liu, Y.; Shen, X.; Gao, H.; Tang, D.; Liu, J. Time series data coupling enhancement method of distributed photovoltaic cluster based on bidirectional recurrent imputation network. *Power Syst. Technol.* **2024**, *48*, 2784–2794.
5. Chen, Y.; Liu, Y.; Yin, H.; Tang, Z.; Qiu, G.; Liu, J. Multiagent Soft Actor–Critic Learning for Distributed ESS Enabled Robust Voltage Regulation of Active Distribution Grids. *IEEE Trans. Ind. Inform.* **2024**, *20*, 11069–11080. [CrossRef]
6. Zhou, D.; Pan, X.; Sun, X.; Hu, F. Resilience Assessment Framework for High-Penetration Renewable Energy Power System. *Sustainability* **2025**, *17*, 2058. [CrossRef]
7. Lu, J.; Fang, S.; Du, C.; Su, J.; Zheng, Y.; Liu, J. Technical challenges and expectation of new rural power grid with high proportion of renewable energy. *Power Demand Side Manag.* **2022**, *24*, 38–43.
8. Kong, X.; Feng, L.; Peng, K.; Song, G.; Xiao, C. Network and Energy Storage Joint Planning and Reconstruction Strategy for Improving Power Supply and Renewable Energy Acceptance Capacities. *Sustainability* **2025**, *17*, 1292. [CrossRef]
9. Yuan, H.; Ye, H.; Chen, Y.; Deng, W. Research on Optimal Configuration of Photovoltaic and Energy Storage in Rural Microgrid. *Guangdong Electr. Power* **2023**, *36*, 49–57. [CrossRef]
10. Yan, Y.; Cheng, Y.; Chen, X. Distribution Network Topology and Coordinated Planning of Storage and Load Resources Adapted to Photovoltaic High Penetration Access. *Guangdong Electr. Power* **2024**, *37*, 50–60.
11. Wang, X.; He, W.; Wu, H.; Zhang, R.; Long, Y.; Wu, J. Aggregation method of flexible resource feasibility domain for promoting distributed photovoltaic consumption in distribution network. *Distrib. Util.* **2024**, *41*, 3–11+20.
12. Zhang, Y.; Chen, C.; Xue, F.; Ma, L.; Zheng, M. Two-stage stochastic optimal voltage control of high-proportional photovoltaic distri-bution networks considering auxiliary power to hydrogen. *Electr. Power* **2024**, *57*, 23–35.
13. Shao, C.; Li, P.; Yang, X.; Liu, Y. Joint planning for energy storage systems and line capacity enhancement of distribution network considering installation area limits of distributed photovoltaic. *Sichuan Electr. Power Technol.* **2023**, *46*, 67–74.
14. Chen, H.; Tang, J.; Wu, H.; Song, J.; Dong, H.; Li, H. Optimal scheduling of distribution network considering electric vehicle demand response and carbon quota revenue. *Power Syst. Technol.* **2025**, 1–12. Available online: https://link.cnki.net/urlid/11.2410.tm.20241030.1000.001. (accessed on 28 May 2025).
15. Zhao, S.; Xu, J.; Teng, X.; Li, Y.; Peng, C.; Yan, L. A low-carbon and economically efficient dispatch model for distribution networks based on carbon emission flow theory. *Zhejiang Electr. Power* **2024**, *43*, 122–132.
16. Wang, W.; Gao, H.; Wang, R.; Li, H.; Liu, J. Distributionally robust optimization of distribution network considering distributed generator support and agricultural facility coordination. *Autom. Electr. Power Syst.* **2023**, *47*, 89–98.
17. Lu, Z.; Lin, Y.; Qiao, Y.; Wu, L.; Xia, X. Flexibility supply-demand balance in power system with ultra-high proportion of renewable energy. *Autom. Electr. Power Syst.* **2022**, *46*, 3–16.
18. Monteiro, R.V.A.; Bonaldo, J.P.; da Silva, R.F.; Bretas, A.S. Electric distribution network reconfiguration optimized for PV distributed generation and energy storage. *Electr. Power Syst. Res.* **2020**, *184*, 106319. [CrossRef]
19. Fu, X.; Zhou, Y.; Sun, H.; Guo, Q. Online security analysis of a park-level agricultural energy internet: Review and prospect. *Proc. CSEE* **2020**, *40*, 5404–5412.
20. Bian, H.; Chen, L.; Ma, F.; Zhang, X.; Jiang, J. Optimal operation strategy based on central decoupling and evolutionary game for multiple agricultural integrated energy systems. *Electr. Power Constr.* **2022**, *43*, 26–36.
21. Jiang, F.; Xiao, C.; Yi, Z.; He, G.; Guo, Q.; Peng, X.; Xiao, G. Multi-energy cooperation and low-carbon operation strategy of eco-agricultural inte-grated energy system containing photovoltaic and biomass energy. *Proc. CSEE* **2024**, *44*, 1352–1364.
22. Wei, Z.; Fu, X.; Zhou, Y.; Yang, F. Comprehensive security analysis of park-level agricultural energy internet considering physiological characteristics of crops. *Power Syst. Technol.* **2022**, *46*, 3406–3416.
23. Yu, L.; Sun, Y.; Yang, S.; Li, X. Autonomous optimization model of village multi-energy system considering energy supply characteristics of waste treatment facilities. *Power Syst. Technol.* **2022**, *46*, 2287–2297.
24. Zhang, J.; Ren, H.; Liu, D.; Zhou, L.; Shao, J.; Jia, Y.; Chen, H. Energy management strategies in agricultural parks considering market clearing. *Electr. Power Constr.* **2024**, *45*, 58–68.
25. Zheng, H.; Zeng, F.; Fu, Y.; Han, C.; Zhang, L.; Dong, L. Bi-level distributed power planning based on E-C-K-means clustering and sop optimization. *Acta Energiae Solaris Sin.* **2022**, *43*, 127–135.
26. Zhang, Y.; Cheng, H. Novel Double Auction Mechanisms for Agricultural Supply Chain Trading. *IEEE Access* **2023**, *11*, 50382–50397. [CrossRef]

27. Schor, N.; Bechar, A.; Ignat, T.; Dombrovsky, A.; Elad, Y.; Berman, S. Robotic Disease Detection in Greenhouses: Combined Detection of Powdery Mildew and Tomato Spotted Wilt Virus. *IEEE Robot. Autom. Lett.* **2016**, *1*, 354–360. [CrossRef]
28. Sun, Y. Study on Structure Optimization and Heat Transfer Characteristics of Stereoscopic Cycle Active Heat Storage System in Solar Greenhouse. Ph.D. Thesis, Northwest A&F University, Xi'an, China, 2020.
29. Chen, H.; Fu, L.; Bai, L.; Jiang, T.; Xue, Y.; Zhang, R.; Chowdhury, B.; Stekli, J.; Li, X. Distribution Market-Clearing and Pricing Considering Coordination of DSOs and ISO: An EPEC Approach. *IEEE Trans. Smart Grid* **2021**, *12*, 3150–3162. [CrossRef]
30. Li, P.; Liu, Y.; Liao, H.; Xu, L.; Xu, X.; Xiang, Y.; Liu, J. Differentiated resilient power supply service and its pricing method of distribution network for extreme events. *Power Syst. Technol.* **2024**, *48*, 4074–4086.

Disclaimer/Publisher's Note: The statements, opinions and data contained in all publications are solely those of the individual author(s) and contributor(s) and not of MDPI and/or the editor(s). MDPI and/or the editor(s) disclaim responsibility for any injury to people or property resulting from any ideas, methods, instructions or products referred to in the content.